Chinese Chemical Letters 33 (2022) 1087–1090

Contents lists available at ScienceDirect

Chinese Chemical Letters

journal homepage: www.elsevier.com/locate/cclet

Multilayer core-shell nanostructures for enhanced 808 nm responsive upconversion

Yao Wang[a,1], Jingxiang Low[a,1], Yafei Bi[a], Yu Bai[a], Yawen Jiang[a], Huihui Wang[a], Weiyong Liu[b,*], Yuqian Ma[a], Yunuo Chen[a], Ran Long[a,*], Yujie Xiong[a,b,*]

[a] *Hefei National Laboratory for Physical Sciences at the Microscale, Frontiers Science Center for Planetary Exploration and Emerging Technologies, School of Chemistry and Materials Science, National Synchrotron Radiation Laboratory, Neurodegenerative Disorder Research Center, CAS Key Laboratory of Brain Function and Disease, and School of Life Sciences, University of Science and Technology of China, Hefei 230026, China*

[b] *Department of Ultrasound, The First Affiliated Hospital of USTC, Division of Life Sciences and Medicine, University of Science and Technology of China, Hefei 230036, China*

ARTICLE INFO

Article history:
Received 17 April 2021
Revised 12 May 2021
Accepted 3 June 2021
Available online 12 June 2021

Keywords:
808 nm excitation
Upconversion nanocrystals
Core-shell structure
Structure construction
Emission enhancement

ABSTRACT

The construction of core-shell structure is an effective strategy for promoting the emission efficiency of upconversion nanocrystals (UCNCs). In this work, the UCNCs based on Nd-doping with a multilayer core-shell nanostructure are fabricated toward achieving efficient upconversion for 808 nm excitation, which have great potential for optical applications, especially photobiological applications.

Lanthanide (Ln)-doped upconversion nanocrystals (UCNCs) have been widely used in plenteous biological applications such as bioimaging, biosensing and drug delivery, owning to its unique features of effective near-infrared (NIR) upconversion, low luminescent background interference, as well as negligible biotoxicity [1–7]. However, water – the vital component of organisms – owns intense absorption in the NIR spectrum around 970 nm, which curbs the optical applications of 980 nm responsive UCNCs [8,9]. For this reason, the Nd-doped UCNCs excited by 808 nm light have recently emerged as next-generation UCNCs for biological applications toward minimizing the overheating risk [10–12]. Nevertheless, Nd^{3+} ions with plenty of complicated energy levels can cause an increase in intrinsic energy loss channels during the nonlinear process in upconverting NIR, because Nd^{3+} and other lanthanide cations are randomly substituted for each other in the lattice of UCNCs. This feature causes complicated energy levels and deleterious cross-relaxation energy transfer (ET), leading to a weak emission performance that restricts their practical usability [13–15].

Considering the negative effect brought by the Nd^{3+} ions, the concentration of Nd^{3+} ions in UCNCs is normally limited to a relatively low level (*ca.* 1%–2%), limiting its function in enhancing the upconversion efficiency. In this context, multilayer core-shell UCNCs with different Ln-doping concentrations are designed to prohibit the negative effect of Nd^{3+} ions and enhance the upconversion emission efficiency [16,17]. In detail, the precise construction of an additional shell containing moderate Nd dopants can effectively isolate the Nd^{3+} ions from other Ln ions in the core (*e.g.*, Er^{3+} and Yb^{3+}), prohibiting the noxious energy transfer from other Ln ions back to Nd^{3+} ions and thus reducing the intrinsic energy loss of Nd^{3+} ions in high concentration [18-20]. Apart from avoiding the intrinsic energy loss, the additional shell can effectively suppress surface quenching during the upconversion process, further enhancing the light emission efficiency [21]. For example, Wang *et al.* demonstrated that the introduction of the $NaGdF_4$ shell can reduce the concentration of the defects, impurities, ligands and solvents on the surface of Yb/Tm co-doped UCNCs, which act as the surface quenching sites for the excitation energies, thereby enhancing the upconversion efficiency of UCNCs [22]. Given these advantages, the construction of the multilayer core-shell nanostructures has emerged as a promising strategy for boosting the upconversion capability of Ln-doped UCNCs.

Herein, we prepare $NaGdF_4$:Nd,Yb,Er@$NaGdF_4$:Nd@$NaGdF_4$ core/shell/shell UCNCs (css-UCNCs) for NIR-upconverted applications. In the core, Er^{3+} (2 mol%), Yb^{3+} (20 mol%) and Nd^{3+} (2 mol%) ions are doped as the emission center, energy transfer

---

[*] Corresponding authors.

E-mail addresses: lwy_ultras@126.com (W. Liu), longran@ustc.edu.cn (R. Long), yjxiong@ustc.edu.cn (Y. Xiong).

[1] These authors contributed equally to this work.

https://doi.org/10.1016/j.cclet.2021.06.007

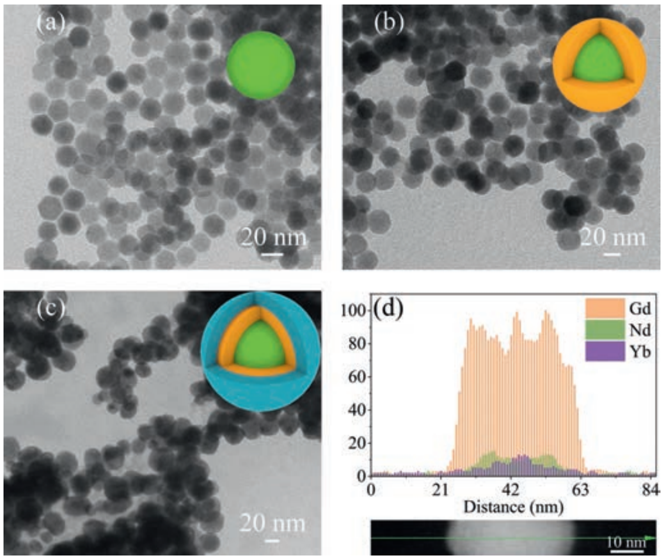

Fig. 1. TEM image of (a) c-UCNCs, (b) cs-UCNCs and (c) css-UCNCs. (d) EDS line scan across a single css-UCNC and the corresponding elemental distribution.

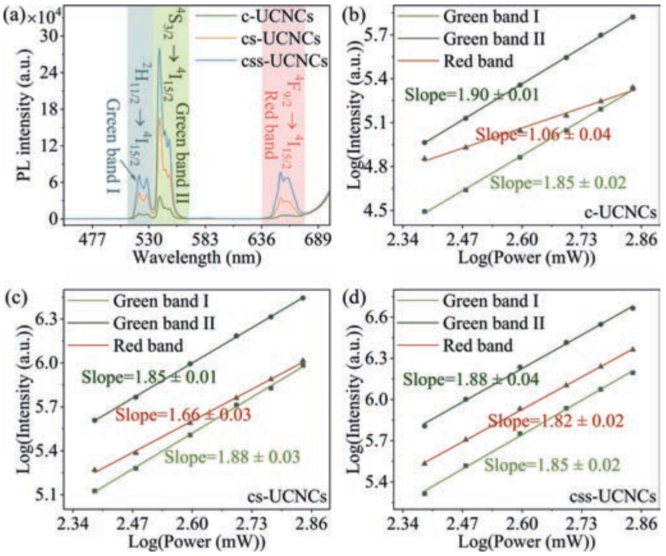

Fig. 2. (a) Upconversion emission spectra under 808 nm laser with the power of 497 mW for c-UCNCs, cs-UCNCs and css-UCNCs. Pump power-dependent upconversion emission of green band I, green band II and red band of Er^{3+} ions in (b) c-UCNCs, (c) cs-UCNCs and (d) css-UCNCs at 808 nm laser with different power densities of 200–700 mW.

bridging and excitation center, respectively. For the inner shell, the Nd^{3+} ions (20 mol%) are doped to allow more photons at 808 nm to be sensitized during the upconversion. For the outer shell, the pristine $NaGdF_4$ is chosen as the protective shell to further reduce the negative effect of surface quenching. Such a work on the fabrication of multilayer core-shell UCNCs toward utilization of NIR photon energy is anticipated to facilitate various applications, especially biological applications.

$NaGdF_4$:Nd,Yb,Er core UCNCs (c-UCNCs) were synthesized according to the previous report [23]. The 6.4 mL lanthanide-oleate complex (0.76 mmol Gd^{3+}, 0.02 mmol Nd^{3+}, 0.20 mmol Yb^{3+} and 0.02 mmol Er^{3+}) were added into 12.8 mL 1-octadecene and stirred for 30 min. Then a methanol solution containing 1 mmol NaOH and 4 mmol NH_4F was transferred to the above mixture, followed by the vacuum at 100 °C for 30 min to remove impurities. The resultant products can be collected after a growth process at 280 °C for 1.5 h. The cyclohexane/alcohol (1:1) solution was then employed to wipe off organic ligands on the surface of UCNCs during centrifuging.

Afterwards, $NaGdF_4$:Nd,Yb,Er@$NaGdF_4$:Nd core/shell UCNCs (cs-UCNCs) were synthesized. 1 mmol c-UCNCs precursors were firstly dispersed in cyclohexane and injected into lanthanide complex (0.8 mmol Gd^{3+} and 0.2 mmol Nd^{3+}) with 6.4 mL oleic acid and 12.8 mL 1-octadecene, followed by the added mixture of NaOH and NH_4F methanol solution. Finally, cs-UCNCs can be collected after the growth process at 280 °C for 1.5 h.

Finally, the core/shell/shell UCNCs (css-UCNCs) can be achieved by introducing an addition $NaGdF_4$ shell on cs-UCNCs. Specifically, 1 mmol cs-UCNCs precursors were firstly dispersed in cyclohexane and added into lanthanide (1 mmol Gd^{3+}) organic complex (oleic acid and 1-octadecene). The final css-UCNCs of $NaGdF_4$:Nd,Yb,Er@$NaGdF_4$:Nd@$NaGdF_4$ can be obtained after the growth process at 280 °C for 1.5 h.

As revealed by the X-ray diffraction patterns in Fig. S1 (Supporting information), all the prepared samples demonstrate the hexagonal phase of $NaGdF_4$ (JCPDS No. 27–0699), suggesting that the $NaGdF_4$ remains unchanged during the doping and multilayer shell loading. Note that lanthanide ions have to be selectively dispersed into different shells during the synthesis to achieve the goal of upconversion emission enhancement under 808 nm excitation. Generally, the UCNCs of $NaGdF_4$:Nd (2 mol%), Yb (20 mol%) and Er (2 mol%) (named as c-UCNCs) are designed as the core. All the dopants play equally important roles in enhancing the upconversion performance of the $NaGdF_4$. Such a model structure is chosen according to the previous works and has been proven to be effective upconversion UCNCs [8,15,24]. In detail, the Nd^{3+} ions can absorb and convert the 808 nm laser into excited photon energy for receptors (Yb and Er) via the excited-state absorption process. In turn, Yb^{3+} ions act as a bridge to modulate energy transfer channels between Nd^{3+} and Er^{3+} ions and cut off the noxious reversed energy loss. Finally, the Er^{3+} ions act as the emission center which accept excited energies from Yb and Nd and further convert them to emission photons [25]. The morphologies of the prepared c-UCNCs are studied *via* transmission electron microscopy (TEM, Fig. 1a), showing their uniform spherical structure with an average size of 18.14 nm (Fig. S2a in Supporting information).

After obtaining the c-UCNCs, the $NaGdF_4$:Nd (20 mol%) is chosen to be loaded onto the c-UCNCs to form a shell for providing more Nd^{3+} ions toward effectively utilizing the 808 nm incident light, increasing the stimulated photon energy for enhancing the upconverted emission [26]. It should be kept in note that the concentration quenching effect on upconversion emission arises with the increase in the concentration of the lanthanide dopants (*i.e.*, Nd^{3+}, Yb^{3+}, Er^{3+} ions) which can result in additional quenching channels and cause efficiency loss by nonradiative relaxation [27,28]. In addition, the high concentration of the Nd^{3+} ions can also lead to an increase in the reversed energy transfer back to Nd, causing the reduction in upconversion ability [29]. For this reason, a moderate doping concentration of Nd (20 mol%) in the additional shell is necessary to avoid the above-mentioned problems. After the introduction of the $NaGdF_4$:Nd on the c-UCNCs, the size of the $NaGdF_4$:Nd,Yb,Er@$NaGdF_4$:Nd (cs-UCNCs) nanostructure is increased to 24.78 nm, 6.64 nm larger than that of c-UCNCs (Fig. 1b and Fig. S2b in Supporting information). Finally, a pristine $NaGdF_4$ shell is further loaded onto the cs-UCNCs to protect the upconversion emission from the negative surface quenching effect. As shown in Fig. 1c and Fig. S2c (Supporting information), the size of such css-UCNCs is further increased to 31.34 nm, suggesting that the $NaGdF_4$ shell owns an average thickness of 6.56 nm.

To have a closer understanding on the composition of the css-UCNCs, the elemental distribution analysis is performed using energy dispersive spectroscopy (EDS). As shown in Fig. 1d and Fig.

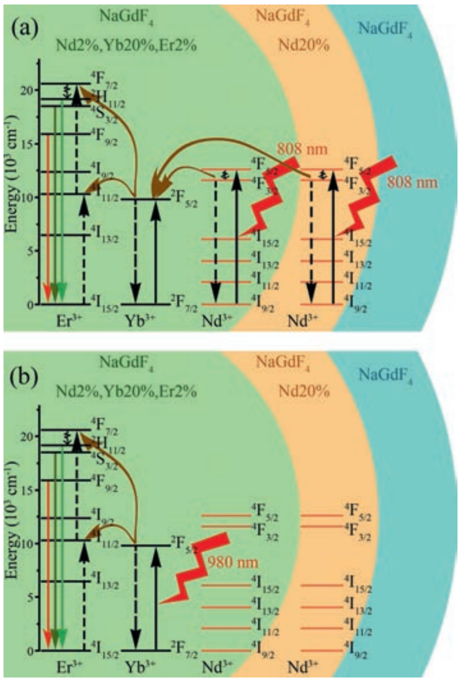

Fig. 3. Schematic illustration for the energy level diagrams of Nd^{3+}, Yb^{3+} and Er^{3+} ions in css-UCNCs under (a) 808 and (b) 980 nm laser excitation.

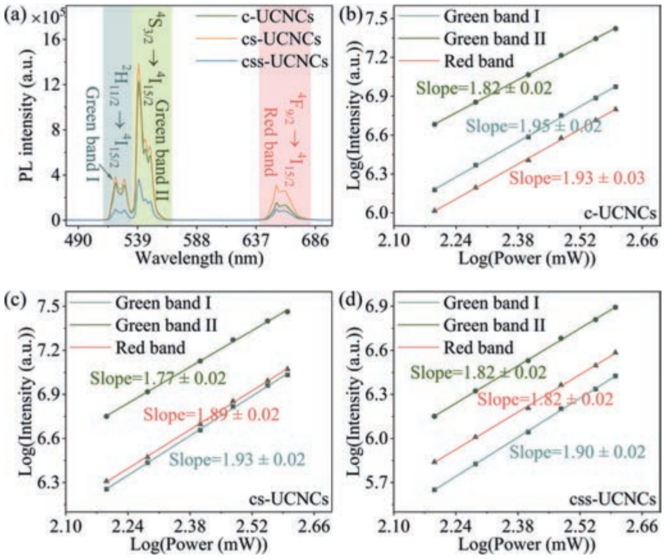

Fig. 4. (a) Upconversion emission spectra under 980 nm laser with the power of 253 mW for c-UCNCs, cs-UCNCs and css-UCNCs. Pump power-dependent upconversion emission of green band I, green band II and red band of Er^{3+} ions in (b) c-UCNCs, (c) cs-UCNCs and (d) css-UCNCs at 980 nm laser with different power densities of 155.5–398 mW.

S3 (Supporting information), the Gd elements exist in the entire core-shell nanostructure, while Nd elements mainly disperse circlewise in the middle shell and the Yb elements are concentrated in the center of the css-UCNCs. Such a distribution of lanthanide elements suggests the successful fabrication of the multilayer core-shell nanostructure according to our design. The formation of multilayer core-shell nanostructure can be further affirmed *via* the elemental mapping profiles as shown in Fig. S4 (Supporting information), which also demonstrate the distribution of the Yb elements in the core of the css-UCNCs.

After manifesting the structure of the css-UCNCs, the photoluminescence (PL) spectroscopy is performed for c-UCNCs, cs-UCNCs and css-UCNCs under 808 nm excitation to investigate their upconversion capability (Fig. 2a). Generally, three main emission bands can be found at 521 nm (green band I), 540 nm (green band II) and 654 nm (red band) for the multilayer core-shell UCNCs, which are attributed to the $^2H_{11/2} \rightarrow {}^4I_{15/2}$, $^4S_{3/2} \rightarrow {}^4I_{15/2}$ and $^4F_{9/2} \rightarrow {}^4I_{15/2}$ transitions of Er^{3+} ion, respectively (Fig. 3a). This suggests that the designed UCNCs are able to upconvert the incident 808 nm light into higher energy photons. Specifically, the Nd^{3+} ions can absorb incident photons and transfer the energies to Er^{3+} ions mediated by Yb^{3+} ions. Interestingly, the intensities of the emission bands are promoted by forming more shell layers. The integral results of PL spectra (Table S1 in Supporting information) show that the emission intensities of cs-UCNCs and css-UCNCs are 4.33 and 7.82 fold higher than that of c-UCNCs, respectively. Such a upconversion performance improvement is enabled by the interplay of two shell layers. The inner shell of $NaGdF_4$:Nd can enhance the utilization efficiency toward the 808 nm excitation, while the outer shell of $NaGdF_4$ substantially avoids the surface quenching effect and further enhances the upconversion efficiency [30]. The observation here confirms that the construction of a multilayer core-shell structure is an effective method for enhancing the upconversion capability of the Ln-doped UCNCs.

Furthermore, we have studied the pump power-dependent upconversion emission capability of the prepared samples as shown in Figs. 2b–d. Typically, PL intensity (I_{PL}) is directly proportional to the P^n (p is pump power and n is the photon number required in the excitation process) [31]. As such, the values of n can be obtained from the slope of $\log I_{PL}$ *versus* $\log P^n$. Clearly, the slopes of green bands (I and II) and red band for all samples show the typical two-photon excitation process. It should be noted that, in comparison with the green bands, the slope values of the red band greatly increase after loading the inner shell and outer shell. This feature is ascribed to the fact that the prepared samples can easily reach the excited state of green bands ($^2H_{11/2}$ and $^4S_{3/2}$) even with the structure with low upconversion efficiency (c-UCNCs) [32]. In contrast, such a low upconversion efficiency of c-UCNCs can hardly populate the excited state of red band ($^4F_{9/2}$), resulting in a low slope value (1.06). After improving the upconversion efficiency *via* increasing the number of shell layers, the red band can be effectively emitted, thereby significantly improving its slope value to 1.66 (cs-UCNCs) and 1.82 (css-UCNCs).

More importantly, differently from the conventional Nd-sensitized process, which can be only initiated at 808 nm excitation, all of our prepared samples can be also excited by the incident 980 nm light through the Yb-sensitized process (Fig. 3b). Similarly to the results obtained under 808 nm excitation, the increase in emission intensity in Fig. 4a can be observed on the cs-UCNCs compared to the c-UCNCs because the $NaGdF_4$:Nd can act as the inert protective shell to minimize the surface quenching of $NaGdF_4$:Nd,Yb,Er core. However, after loading the outer shell, the emission intensity is reduced as only the Yb dopants in the core of css-UCNCs can respond to the 980 nm stimulation and the double shells with a total thickness of 13.2 nm momentously scatter the emitted and incident light [33]. The power-dependent emission test is also performed under 980 nm excitation for different prepared samples. Figs. 4b–d indicate the similar two-photon excitation process of $^2H_{11/2}$ (green band I), $^4S_{3/2}$ (green band II) and $^4F_{9/2}$ (red band) intermediate levels on all the prepared samples. As shown in Table S2 (Supporting information), the proportion of the red band significantly is promoted with increasing shell layers. This feature is quite straightforward as the longer emission wavelength of the red band compared to the green bands can result in a lower scattering of emitted light.

In summary, we have successfully designed and synthesized novel multilayer core-shell nanostructures for upconversion applications. The optimized css-UCNCs demonstrate superior upconversion capability toward incident 808 nm light for emitting green band and red band light. The underlying mechanism for enhanced upconversion capability on css-UCNCs is further proposed. Specifically, the Er^{3+} (2 mol%), Yb^{3+} (20 mol%) and Nd^{3+} (2 mol%) ions in the core act as the emission center, bridging inverter and excited center, respectively. The inner shell consisting of Nd^{3+} (20 mol%) ions boosts the light utilization ability of the UCNCs, while the outer shell of pristine $NaGdF_4$ reduces the surface quenching effect. We expect that this work can herald the advent for the construction of efficient multilayer core-shell UCNCs for various upconversion applications, especially in biological applications.

Declaration of competing interest

The authors declare that they have no competing financial interest.

Acknowledgments

This work was financially supported in part by National Key R&D Program of China (Nos. 2020YFA0406103, 2017YFA0207301), NSFC (Nos. 21725102, 91961106, U1832156, 22075267), Science and Technological Fund of Anhui Province for Outstanding Youth (No. 2008085J05), Youth Innovation Promotion Association of CAS (No. 2019444), Young Elite Scientist Sponsorship Program by CAST, China Postdoctoral Science Foundation (Nos. BH2340000099, BH2340000138), and Users with Excellence Program of Hefei Science Center CAS (No. 2020HSC-UE003). We thank the support from USTC Center for Micro- and Nanoscale Research and Fabrication.

Supplementary materials

Supplementary material associated with this article can be found, in the online version, at doi:10.1016/j.cclet.2021.06.007.

References

[1] L. Francés-Soriano, N. Peruffo, M.M. Natile, N. Hildebrandt, Analyst 145 (2020) 2543–2553.
[2] D. Ling, H. Li, W. Xi, et al., J. Mater. Chem. B 8 (2020) 1316–1325.
[3] L. Gong, S. Liu, Y. Song, et al., J. Mater. Chem. B 8 (2020) 5952–5961.
[4] G. Liu, F. Jiang, Y. Chen, et al., Nanomedicine 24 (2020) 102135.
[5] K. Du, X. Xu, S. Yao, et al., CrystEngComm 20 (2018) 1945–1953.
[6] B. Liu, C. Li, P. Yang, et al., Adv. Mater. 29 (2017) 1605434.
[7] Y. Dai, H. Bi, X. Deng, et al., J. Mater. Chem. B 5 (2017) 2086–2095.
[8] L.M. Wiesholler, F. Frenzel, B. Grauel, et al., Nanoscale 11 (2019) 13440–13449.
[9] J.P. Wold, M. O'Farrell, J. Tschudi, et al., J. Food Eng. 277 (2020) 109921.
[10] Z. Hou, K. Deng, M. Wang, et al., Chem. Mater. 31 (2019) 774–784.
[11] Y. Wang, G. Liu, L. Sun, et al., ACS Nano 7 (2013) 7200–7206.
[12] Z. Hou, K. Deng, C. Li, et al., Biomaterials 101 (2016) 32–46.
[13] W. Yao, Q. Tian, B. Tian, et al., Sci. China Mater. 62 (2019) 368–378.
[14] Z. Ba, Y. Zheng, M. Hu, et al., CrystEngComm 21 (2019) 4175–4183.
[15] X. Huang, J. Lin, J. Mater. Chem. C 3 (2015) 7652–7657.
[16] X. Lin, X. Chen, W. Zhang, et al., Nano. Lett. 18 (2018) 948–956.
[17] C. Cheng, Y. Xu, G. De, et al., CrystEngComm 22 (2020) 6330–6338.
[18] B. Zhou, B. Tang, C. Zhang, et al., Nat. Commun. 11 (2020) 1174.
[19] F. Zhang, R. Che, X. Li, et al., Nano. Lett. 12 (2012) 2852–2858.
[20] Z. Lei, X. Ling, Q. Mei, et al., Adv. Mater. 32 (2020) 1906225.
[21] Y. Zhang, Y. Cao, Y. Zhao, et al., J. Am. Ceram. Soc. 104 (2020) 361–368.
[22] F. Wang, J. Wang, X. Liu, Angew. Chem. Int. Ed. 49 (2010) 7456–7460.
[23] F. Wang, R. Deng, X. Liu, Nat. Protoc. 9 (2014) 1634–1644.
[24] Z. Nie, X. Ke, D. Li, et al., J. Phys. Chem. C 123 (2019) 22959–22970.
[25] C. Liu, B. Liu, J. Zhao, et al., Angew. Chem. Int. Ed. 59 (2020) 2634–2638.
[26] X. Xie, N. Gao, R. Deng, et al., J. Am. Chem. Soc. 135 (2013) 12608–12611.
[27] Z. Wang, A. Meijerink, J. Phys. Chem. C 122 (2018) 26298–26306.
[28] B. Chen, F. Wang, Acc. Chem. Res. 53 (2019) 358–367.
[29] Y. Qin, Z. Dong, D. Zhou, et al., Opt. Mater. Express 6 (2016) 1942–1955.
[30] Y. Liu, Y. Lu, X. Yang, et al., Nature 543 (2017) 229–233.
[31] M. Pollnau, D.R. Gamelin, S. Lüthi, et al., Phys. Rev. B 61 (2000) 3337–3346.
[32] Y. Lei, H. Song, L. Yang, et al., J. Chem. Phys. 123 (2005) 174710.
[33] Y. Hu, Q. Shao, Y. Dong, J. Jiang, J. Phys. Chem. C 123 (2019) 22674–22679.